



## Ptarmigan Fiord basement-cover thrust imbricates, Baffin Island, Nunavut

T.C. Chadwick<sup>1</sup>, M.R. St-Onge<sup>2</sup>, O.M. Weller<sup>2</sup>, S.D. Carr<sup>1</sup> and B.J. Dyck<sup>3</sup>

<sup>1</sup>Ottawa-Carleton Geoscience Centre, Carleton University, Ottawa, Ontario, [timchadwick@cmail.carleton.ca](mailto:timchadwick@cmail.carleton.ca)

<sup>2</sup>Natural Resources Canada, Geological Survey of Canada, Ottawa, Ontario

<sup>3</sup>Department of Earth Sciences, University of Oxford, Oxford, United Kingdom

*This work is part of the larger South Baffin mapping project, a partnership between the Canada-Nunavut Geoscience Office (CNGO) and Natural Resources Canada's (NRCan) Geo-mapping for Energy and Minerals (GEM) program on Baffin Island. This particular mapping project is being led by the Geological Survey of Canada (GSC) in collaboration with CNGO, the Government of Nunavut, Nunavut Arctic College, Carleton University and Oxford University. Logistical support is provided by the Polar Continental Shelf Project and several local, Inuit-owned businesses. The study area comprises all or parts of six 1:250 000 map areas north of Iqaluit (NTS areas 26B, C, F, G, J and K). The objective of the work is to complete the regional bedrock mapping for the southern half of Baffin Island and provide a new, modern, geoscience understanding of this part of eastern Nunavut.*

---

Chadwick, T.C., St-Onge, M.R., Weller, O.M., Carr, S.D. and Dyck, B.J. 2015: Ptarmigan Fiord basement-cover thrust imbricates, Baffin Island, Nunavut; in Summary of Activities 2015, Canada-Nunavut Geoscience Office, p. 61–72.

### Abstract

The rocks at Ptarmigan Fiord on the Hall Peninsula of Baffin Island underwent midcrustal deformation during the formation of the Paleoproterozoic Trans-Hudson Orogen. The structural style in the region is dominated by imbricate panels of Archean basement orthogneiss and Paleoproterozoic supracrustal strata, interpreted to have been deformed by thick-skinned ductile thrusting. Basement rocks comprise amphibolite-facies metatonalite, metagranodiorite, metaquartz-diorite and metamonzogranite, and cover rocks comprise amphibolite-facies migmatitic pelitic and semipelitic schist, psammitic schist, amphibolite, calcsilicate and quartzite. The  $S_{1a}$  penetrative foliation is variably present in basement rocks and consistently present in cover rocks, and is defined by alignment of biotite, sillimanite and leucogranite that formed before and during the thermal metamorphic peak. The  $S_{1a}$  foliation was deformed by  $F_{1b}$  isoclinal folds with an amplitude of 100 m. These structures are interpreted as forming during a  $D_1$  east-west crustal shortening event. Basement and cover imbrication occurred after the thermal metamorphic peak and is interpreted as  $D_2$  thick-skinned ductile thrusting. Ductile thrust faults at the base of seven basement-cover slices are identified on the basis of repetition of units and strain localization, and are interpreted as predominantly south-to-southeast verging on the basis of shear-sense indicators. There are two structural panels of  $D_2$  thrust imbricates, one in the northwestern part of the map area and one in the eastern part of the map area. Map-scale crosscutting relationships indicate that the northwestern panel overthrust the eastern panel on a southeasterly  $T_{2c}$ -directed thrust fault, following a  $F_{2b}$  folding event that folded the  $T_{2a}$  basement-cover thrust imbricates in the eastern panel. The Ptarmigan Fiord area contains a world-class exposure of thick-skinned structures as they are spectacularly delineated by belts of distinctive grey-weathering Archean basement rocks and brown- to black-weathering Paleoproterozoic supracrustal rocks.

### Résumé

Les roches de Ptarmigan Fiord dans la péninsule Hall de l'île de Baffin documentent des événements de la déformation de la croûte moyenne survenue au moment de l'orogénèse trans-hudsonienne. Le style de déformation dans la région est dominé par des panneaux imbriqués d'orthogneiss du socle archéen et de strates supracrustales du Paléoprotérozoïque, interprétés comme étant le résultat de chevauchements ductiles de couches épaisses. Le socle comprend les unités du faciès des amphibolites suivantes : métatonalite, métagranodiorite, métadiorite quartzique et métamonzogranite ; les roches de couverture du faciès des amphibolites comprennent, elles, du schiste pélitique et semi-pélitique migmatitique, du schiste psammitique, de l'amphibolite, des silicates calciques et du quartzite. Les roches de couverture sont caractérisées par la présence généralisée d'une foliation  $S_{1a}$ , tandis que cette dernière ne se manifeste que de façon variable dans les roches du socle. Cette foliation est en outre définie par l'alignement de la biotite, de la sillimanite et du leucogranite, qui se sont formés avant et

---

*This publication is also available, free of charge, as colour digital files in Adobe Acrobat® PDF format from the Canada-Nunavut Geoscience Office website: <http://cngo.ca/summary-of-activities/2015/>.*

pendant le pic de métamorphisme thermique. Des plis isoclinaux  $F_{1b}$  ont ensuite imprimé à la foliation  $S_{1a}$  une déformation dont l'amplitude atteint 100 m. Ces structures sont interprétées comme étant le résultat d'un événement de raccourcissement crustal  $D_1$  orienté est-ouest. L'imbrication des roches du socle et des roches de couverture s'est produite après le pic de métamorphisme thermique et est interprétée comme étant le résultat d'un chevauchement ductile de couche épaisse  $D_2$ . Des failles de chevauchement à la base de sept écailles constituées de roches du socle et de couverture ont été repérées grâce à la répétition d'unités et à la localisation des déformations ; en outre, les indicateurs de sens de cisaillement semblent indiquer que le transport tectonique s'est produit généralement en direction sud à sud-est. Il y a deux domaines structuraux de chevauchements  $D_2$ , l'un dans la partie nord-ouest et l'autre dans la partie est de la zone d'étude. Les relations géométriques de recoupement à l'échelle de la carte révèlent que le domaine au nord-ouest a chevauché le domaine à l'est le long d'une faille de chevauchement  $T_{2c}$  à vergence sud-est. Le chevauchement  $T_{2c}$  s'est produit après un épisode de plissement  $F_{2b}$  des panneaux imbriqués  $T_{2a}$  de roches du socle et de couverture dans le domaine de l'est. La région de Ptarmigan Fiord est caractérisée par la présence d'affleurements de premier ordre de structures de chevauchement de couches épaisses que délimitent de façon spectaculaire des bandes distinctes de roches du socle d'âge archéen, auxquelles l'altération a conféré une teinte grisâtre, et de roches supracrustales d'âge paléoproterozoïque, à surface altérée brune et noire.

---

## Introduction

Ptarmigan Fiord is located on western Hall Peninsula, South Baffin Island, Nunavut (Figure 1, inset map). The Hall Peninsula block, the setting of the Ptarmigan study area, is located in the Quebec-Baffin segment of the Paleoproterozoic Trans-Hudson Orogen (THO), a collisional belt that formed during the amalgamation of the supercontinent Nuna (also called Columbia), between 2.0–1.8 Ga (Hoffman, 1988; Lewry and Collerson, 1990; St-Onge et al., 2007; Corrigan, 2012). In the THO, the lower plate comprises the Superior craton whereas the upper plate consists of a collage of Archean crustal fragments, ribbon microcontinents and oceanic arc terranes. The Quebec-Baffin domain is situated in the upper Churchill plate, and includes the Rae craton, Meta Incognita microcontinent and Narsajuaq arc terrane, which were accreted to the southeastern Rae margin between ca. 1.88 and 1.84 Ga (St-Onge et al., 2009). The lower-plate Superior craton terminal collision occurred between ca. 1.82 and 1.80 Ga (St-Onge et al., 2006). The Hall Peninsula block, located east of the Meta Incognita microcontinent (Figure 1), is a section of continental crust composed of tonalitic to monzogranitic Archean basement gneiss and minor supracrustal rocks.

Hall Peninsula was initially mapped by Blackadar (1967), Scott (1999) and in 2012–2014, by the Canada-Nunavut Geoscience Office (CNGO), as part of the Hall Peninsula Integrated Geoscience Project (Steenkamp and St-Onge, 2014). Ptarmigan Fiord was targeted during the summer of 2015, by the Geological Survey of Canada (GSC), as part of a regional bedrock mapping project focused on the central part of Baffin Island (Weller et al., 2015), within the Natural Resources Canada's (NRCan) Geo-mapping for Energy and Minerals (GEM) Program. The purpose of this field-based study is to gain a better understanding of the structural style and tectonic history of the Ptarmigan Fiord area. Mapping at 1:80 000 scale in an approximately 10 by 18 km

area forms the basis of the M.Sc. thesis project by the first author at Carleton University. In this paper, results are presented from the 2015 field season that focus on characterizing the tectonostratigraphy, structures and relative timing of structures with respect to metamorphism in the Ptarmigan Fiord area.

## Geological setting of Hall Peninsula

The bedrock geology of Hall Peninsula includes Archean crystalline basement orthogneiss nonconformably overlain by middle Paleoproterozoic supracrustal cover strata; in the western peninsula, the supracrustal rocks are intruded by orthopyroxene-bearing diorite to monzogranite (Steenkamp and St-Onge, 2014). The basement orthogneiss comprises dominantly gneissic, migmatitic tonalite to monzogranite with local pods of amphibolite and crosscutting syenogranite dykes (op. cit.; From et al., 2014). A crystalline basement sample of K-feldspar porphyritic monzogranite collected from the southeastern part of Ptarmigan Fiord (R003, Figure 1), yielded a zircon U-Pb age of 2719 ± 4 Ma (Rayner, 2014). The supracrustal package is characterized by a larger compositional variation in the eastern part of the peninsula, compared to that in the west (Steenkamp and St-Onge, 2014). The supracrustal rocks consist of upper-amphibolite to lower-granulite facies clastic and pelitic migmatitic schist and gneiss, and compositionally variable amphibolite, calcsilicate and meta-ironstones. The base of the package comprises a blue-grey quartzite, which is overlain by a rusty brown-weathering unit of alternating psammitic, semipelitic and pelitic metasedimentary rocks. Above the basal strata lies a layered unit of semipelitic schist, calcsilicate, meta-ironstone and compositionally variable amphibolite. The amphibolite is interpreted as a sequence of metamorphosed volcanoclastic rocks with minor subaerial mafic volcanic flows (MacKay et al., 2013; MacKay and Ansdell, 2014; Steenkamp and St-Onge, 2014). Approximately 20 km west of Ptarmigan Fiord the



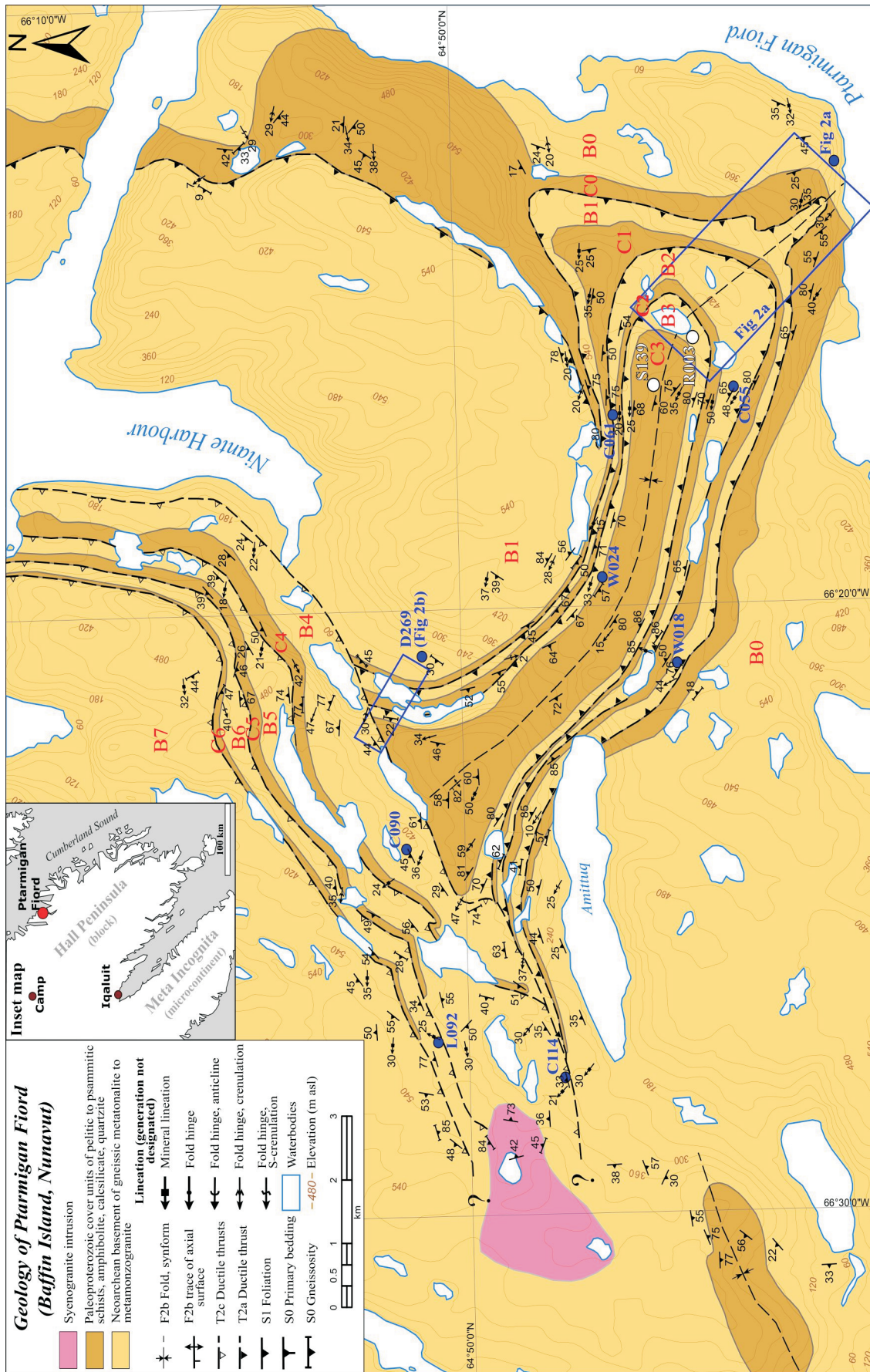


**Figure 1:** Geology of the Ptarmigan Fjord field area on Hall Peninsula of Baffin Island, southeastern Nunavut (scale 1:80 000), showing folded Archean basement (gold colour, B0-B7) and Paleoproterozoic cover (brown colour, C0-C6) imbrications with late (?) syenogranite intrusion (pink). White circles are geochronology sample locales, and blue station numbers show locations of kinematic indicators and panorama photographs; location of Figure 2a and b also shown. Inset map shows location of the field area.

supracrustal rocks transition to a more homogeneous composition, and comprise dominantly pelitic and psammitic metasedimentary units. The transition from clastic and psammitic-pelitic units with mafic lenses, interpreted as margin-proximal supracrustal units, in the east, to mostly deep-water, distal pelitic units, in the west, has been interpreted as a progressive change in paleodepositional environment of supracrustal rocks now exposed on Hall Peninsula (Steenkamp and St-Onge, 2014). A sample of psammitic schist from Ptarmigan Fiord (S139, Figure 1) yielded a significant population of 1.96 Ga zircon grains, indicating a maximum age of deposition at  $1967 \pm 8$  Ma (op. cit.) for that part of the supracrustal package.

Dyck and St-Onge (2014) proposed that three major Paleoproterozoic deformation events characterize the structural and metamorphic evolution of Hall Peninsula, including the Ptarmigan Fiord area. The nature and relative timing of the deformation events are summarized in Table 1.

In the Ptarmigan Fiord area, D<sub>2</sub> thrust repetitions of less than one kilometre thick basement-cover slices dominate the map pattern (Figures 1, 2).

### Bedrock geology of Ptarmigan Fiord map area

There are three map units (Figure 1) in the Ptarmigan Fiord area: 1) Neoproterozoic orthogneiss basement, 2) Paleoproterozoic supracrustal cover rocks, and 3) weakly foliated syenogranite intrusions. Although most of the rocks in the Ptarmigan Fiord area are penetratively metamorphic rocks, the prefix ‘meta’ is omitted from the following lithological descriptions for brevity.

### Neoproterozoic basement lithology

The Neoproterozoic crystalline basement at Ptarmigan Fiord comprises multiple phases of variably deformed gneissic to massive tonalite, quartz diorite, granodiorite and monzogranite (Figure 1). Biotite, hornblende±orthopyroxene tonalite is typically fine to medium grained, weathers light to dark grey, and has a flecked salt and pepper grey colour on the fresh surface. In places, the tonalite gneiss contains 20–150 cm thick blocky to banded lenses and folded bands (Figure 3a).

The mafic lenses, blocks and bands consist of biotite, hornblende, garnet±clinopyroxene quartz diorite. Biotite, hornblende±orthopyroxene granodiorite is typically fine to medium grained, weathers a light grey brown, and contains blocky lenses of quartz diorite. The biotite and hornblende-bearing monzogranite is typically reddish-grey to light brown on the weathered and fresh surfaces, medium to coarse grained in areas of lower strain, and generally contains 5–10 mm elongated and rounded K-feldspar porphyroclasts (Figure 3b).

**Table 1:** Deformation events, structures and metamorphism, Ptarmigan Fiord, Hall Peninsula, Nunavut. Modified after Dyck and St-Onge (2014).

Event	Description
<b>D<sub>0</sub> Predeformation fabric</b>	
S <sub>0</sub>	Gneissic banding in Archean basement rocks Primary bedding
<b>D<sub>1</sub> East-west crustal shortening (pre-synthermal peak)</b>	
F <sub>1a</sub>	Isoclinal folding of S <sub>0</sub>
S <sub>1a</sub>	Metamorphic minerals axial planar to F <sub>1a</sub>
F <sub>1b</sub>	Isoclinal folding of S <sub>1a</sub>
S <sub>1b</sub>	Cleavage axial planar to F <sub>1b</sub>
<b>D<sub>2</sub> Southeast-northwest crustal shortening (post-thermal peak)</b>	
T <sub>2a</sub>	Thick-skinned thrusting in eastern domain
S <sub>2</sub>	Shear fabric oriented parallel to T <sub>2</sub> thrust plane
L <sub>2</sub>	Mineral stretching and elongate growth
F <sub>2b</sub>	Upright folding of T <sub>2a</sub> thick-skinned thrusting
T <sub>2c</sub>	Thick-skinned thrusting in northwestern domain
<b>D<sub>3</sub> North-south crustal shortening</b>	
F <sub>3</sub>	Open folding of T <sub>2a</sub> and T <sub>2c</sub> thick-skinned thrusting

### Paleoproterozoic cover lithology

Stratigraphy within the Paleoproterozoic supracrustal cover rocks is disrupted by multiple deformation events, but estimated to be a minimum of ~200 to 500 m thick. From structurally lowest to highest, the cover succession contains pelitic and semipelitic schist, psammitic schist, amphibolite, calcsilicate and quartzite. This sequence has been mapped on the ground in cover slices ‘C0’ and ‘C1’ on the northern limb of the syncline in the central part of the area, and marker units are traced across the map area (Figures 1, 2). The majority of the supracrustal successions in the study area are truncated above the amphibolite unit by the crystalline basement hanging wall of the overriding thrust imbricate. Rarely are the calcsilicate and quartzite that lie above the amphibolite observed in the cover slices.

### Pelitic and semipelitic schist

The migmatitic garnet–sillimanite–K-feldspar±muscovite pelitic schist and the muscovite-biotite semipelitic schist weather a rusty brown colour and typically occur as 5–20 m thick interlayers within psammite (Figure 3c, d). The sillimanite typically occurs as 1–2 cm long elongate knots with quartz and K-feldspar. In cover sequences ‘C3’–‘C6’ (Figure 1), thin alternating sequences (10–50 cm thick) of pelitic schist and psammitic schist exhibit both sharp and gradational contacts (Figure 3e). These alternating interlayers are interpreted as primary bedding, termed S<sub>0</sub>.

In the eastern part of the study area, within the cover sequences ‘C0’ and ‘C1’ (Figure 1), 1–3 m wide layers of gar-



net-muscovite-sillimanite schist are studded with 5–20 mm diameter garnets (Figure 3f) and are distinctive marker units. Leucogranite veins and dykes, 1–10 cm thick, occur in the pelitic rocks of cover sequences ‘C3’–‘C6’ (Figure 1b). The leucogranite contains millimetre- to centimetre-sized lilac-coloured garnets with mats of fine sillimanite needles. The leucogranite veins crosscut the

dominant  $S_{1a}$  foliation and are aligned within the  $S_{1b}$  axial-planar surface of  $F_{1b}$  isoclinal folds (Figure 3e).

### *Psammitic schist*

Fine- to medium-grained muscovite- and biotite-bearing psammitic schist occurs stratigraphically above the pelitic and semipelitic schist, in 2 to 10 m thick layers. It contains

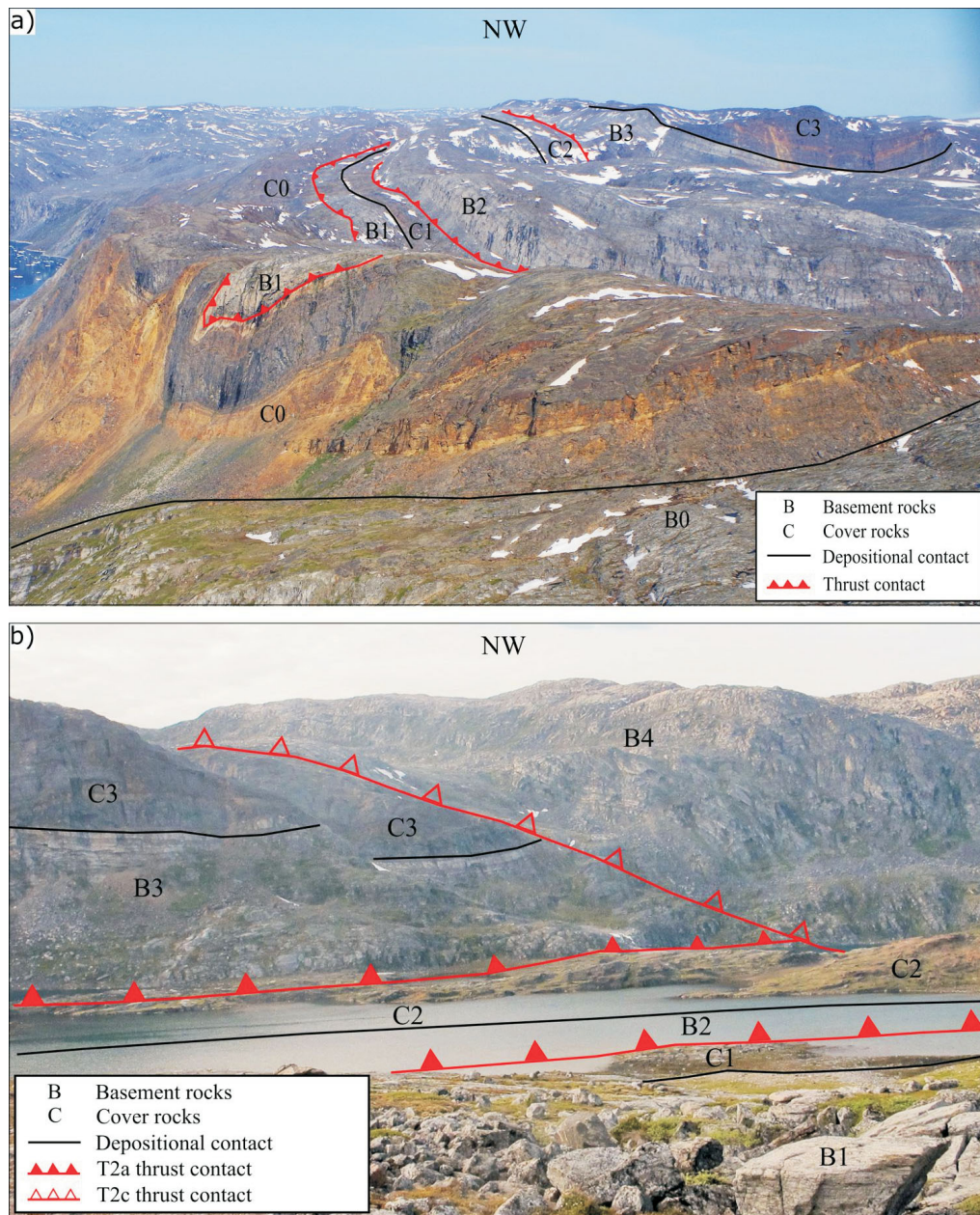


**Figure 2:** Panoramas of Ptarmigan Fiord geology, Hall Peninsula of Baffin Island. The areas covered by the photographs are delineated on Figure 1: **a)** northwestward view facing  $\sim 300^\circ$  azimuth. The photograph is taken from the helicopter above the station labelled ‘Fig 2a’ on Figure 1. Basement rocks are grey, metasedimentary clastic and pelitic cover rocks are brown, and metavolcanic rocks are dark grey. Basement-cover imbricates in the far distance (‘B3’ and ‘C3’) occur in the southeast closure of an upright syncline (Figure 1); **b)** northwestward view facing  $\sim 300^\circ$  azimuth viewed from station D269 (Figure 1) at the boundary between the northwest structural domain and the eastern domain, where a stack of  $T_{2c}$  basement-cover thrust imbricates, with ‘B4’ at the base, truncates  $T_{2a}$  basement-cover imbricates (‘B3’+‘C3’ and ‘B2’+‘C2’) of the eastern domain.



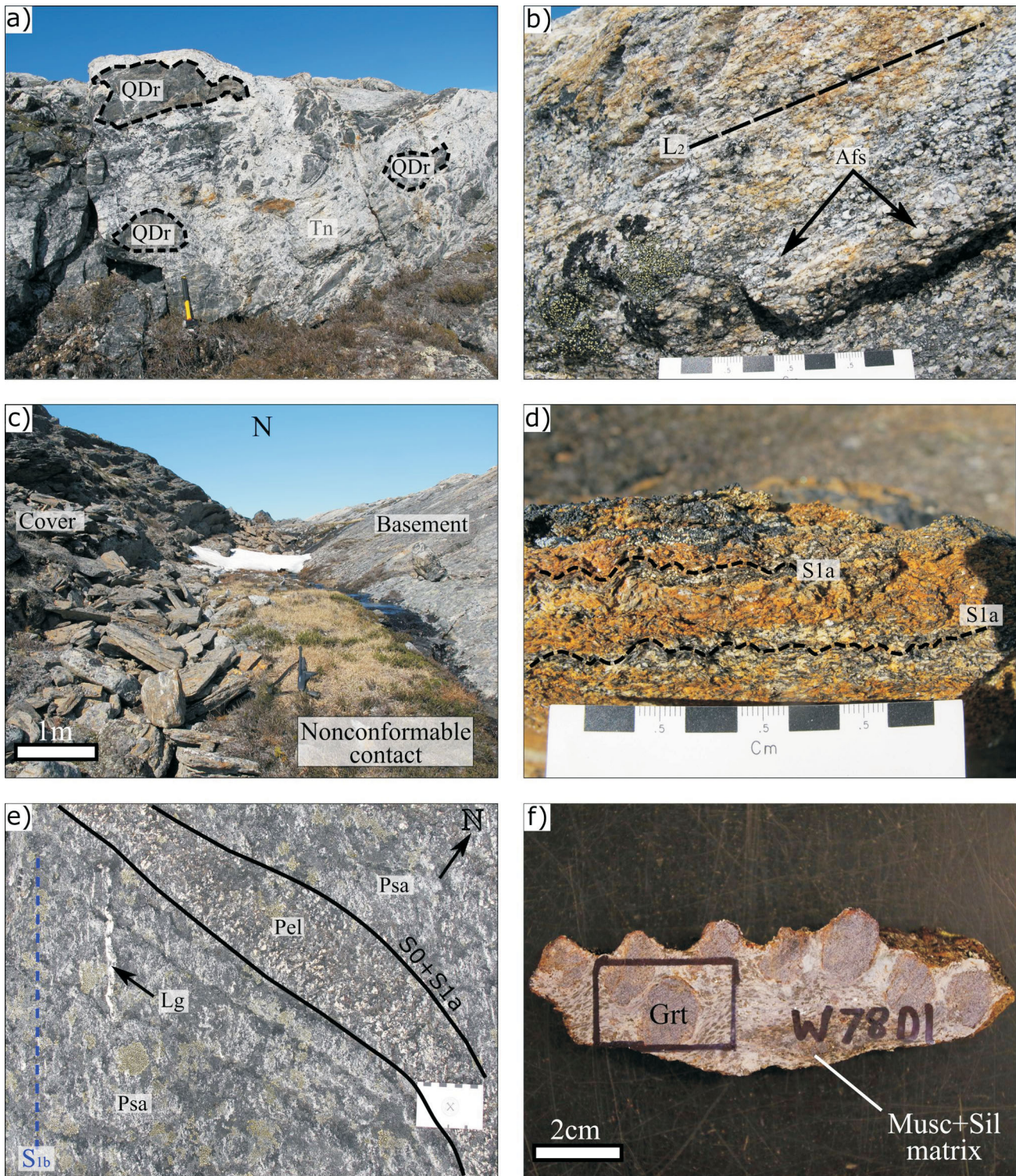


**Figure 3:** Examples of lithology and structure, Ptarmigan Fiord, Hall Peninsula of Baffin Island: **a)** northward view of Neoproterozoic basement tonalite with blocks and layers of quartz diorite (note the 30 cm long hammer for scale); **b)** northward view of Neoproterozoic basement monzogranite with rounded K-feldspar porphyroclasts and  $L_2$  lineation; **c)** northward view of contact between Neoproterozoic basement (right) and Paleoproterozoic supracrustal rocks (left) interpreted as a nonconformable contact (note the 60 cm long Remington 870 for scale); **d)** muscovite-biotite semipelitic schist with primary compositional layering concordant with  $S_{1a}$  is defined by alignment of muscovite and biotite; **e)** psammitic and pelitic garnet-sillimanite-K-feldspar-muscovite schist. Compositional layering, interpreted as primary bedding ( $S_0$ ), is at a high angle to  $S_{1b}$  foliation, parallel to  $F_{1b}$  folds, defined by sillimanite and K-feldspar knots, muscovite and biotite minerals and garnet quartzofeldspathic veins; **f)** garnet-muscovite-sillimanite schist studded with 5–20 mm diameter garnets. Abbreviations: Afs, alkali feldspar; Grt, garnet; Lg, leucogranite veins; Musc, muscovite; Pel, pelitic schist; Psa, psammitic schist; QDr, quartz diorite; Sil, sillimanite; Tn, tonalite.



rare elongate sillimanite–quartz–K-feldspar knots and 1–2 mm sized garnet. The psammitic schist may have interlayers of pelitic schist, with 1 to 3 cm thick gradational contacts.

### ***Amphibolite***

A fine- to medium-grained, black- to dark green-weathering garnet-biotite ( $\pm$ quartz, clinopyroxene) amphibolite unit, up to 30 m thick, typically occurs above the pelitic and psammitic schist units. There are calcite and dolomite infills that are interpreted as interflow and/or pillow selvages. The protolith of the amphibolite is interpreted to be mafic volcanic rocks (Figure 4a).

### ***Calcsilicate***

Thin, 40–200 cm thick layers of white- to dark grey-weathering calcsilicate overlie the amphibolite. The calcsilicate often contains 2–5 cm size tremolite knots within a dolomitic matrix. Tremolite is aligned within the  $S_{1a}$  foliation and within the axial planes of  $F_{1b}$  minor isoclinal folds (Figure 4b).

### ***Quartzite***

A 3 to 10 m thick, fine- to medium-grained, grey-blue weathering quartzite caps the cover units. Quartzite also occurs as 20–50 cm thick lenses within the psammitic schist. It rarely contains relic heavy-mineral bands that define primary bedding and crossbedding. There are 5–20 mm thick biotite- and amphibole-rich mafic layers interbedded within the quartzite that are interpreted as mafic-volcanic ash layers.

## **Syenogranite intrusions**

A red- to pink-weathering, medium-grained, biotite syenogranite pluton occurs near the western margin of the map area (Figure 1). The weakly foliated syenogranite crosscuts the gneissic foliation within the basement rocks (Figure 4c), and is therefore younger than the basement granitoids and the foliation. One- to two-metre thick syenogranite and pegmatite dykes of this suite also occur within the basement and cover imbricates in the central and eastern part of the map area ('B1'+ 'C1' to 'B3'+ 'C3' on Figure 1), but crosscutting relationships involving the intrusions and basement-cover contacts were not observed. The age of the intrusion may provide a timing constraint on the youngest stages of regional deformation.

## **Structural observations and interpretations from Ptarmigan Fiord**

Using the framework developed by Dyck and St-Onge (2014), as summarized in Table 1, structural mapping in the Ptarmigan Fiord area resulted in the identification of three deformation events. There are two structural domains in the map area (Figure 1). The northwestern map domain is char-

acterized by a generally north- to northwest-dipping panel of basement and cover imbricates ('B4'+ 'C4' to 'B7'—the structurally highest basement in the map area) separated by  $T_{2c}$  thrusts. The map pattern of the eastern domain, between Amittuq and Niante Harbour, is dominated by the keel of a  $F_{2b}$  syncline that folds basement-cover  $T_{2a}$  thrust imbricates ('B0'+ 'C0' to 'B3'+ 'C3'), and is readily visible from the air as shown in panorama photo of Figure 2a.

### ***D<sub>1</sub>: East-west crustal shortening (pre-synthermal peak)***

Early Paleoproterozoic deformation ( $D_1$ ) resulted in a strong foliation ( $S_{1a}$ ), axial planar to  $F_{1a}$  folds, which is defined by the alignment of muscovite, biotite and sillimanite in pelitic rocks (Figure 3d). This foliation formed during regional  $F_{1a}$  isoclinal folding. The  $F_{1a}$  folds have ~100 m amplitudes and are generally west-dipping ( $\sim 180^\circ/65^\circ W$ ) with shallow north- and south-plunging fold axes (Dyck and St-Onge, 2014). Throughout the study area the  $S_{1a}$  foliation, primary bedding, leucogranite pods and centimetre-wide leucogranite veins are all folded at the outcrop scale by  $F_{1b}$  isoclinal folds (Figure 4d). The  $F_{1b}$  folds have approximately northwest-trending ( $310\text{--}340^\circ$ ) fold hinges that plunge  $\sim 50^\circ$ , and have west-dipping axial planes oriented  $\sim 140^\circ/75^\circ W$ . An axial planar cleavage ( $S_{1b}$ ) is developed as a result of the  $F_{1b}$  folding (Figure 4d). The axial planar cleavage is best seen in the folded centimetre-wide leucogranite veins and pods as fine fractures, as well as leucogranite veins oriented parallel to the axial plane of the  $F_{1b}$  isoclinal folds (Figure 3e), suggesting that peak metamorphism was syndeformational with this folding event.

### ***D<sub>2</sub>: Southeast-northwest crustal shortening (post-thermal peak) and thick-skinned deformation***

The 100–800 m thick slices of basement and cover rocks are imbricated (Figures 1, 2). On the map (Figure 1) and panorama photographs (Figure 2), seven basement ('B') and cover ('C') imbricates are labelled in structurally ascending order from the deepest structural level ('B1'+ 'C1') to the highest structural level ('B7'). Figure 2a shows the structurally deepest autochthonous basement and overlying cover in the foreground ('B0'+ 'C0') structurally overlain by basement-cover pairs ('B1'+ 'C1' to 'B3'+ 'C3'). Figure 2b shows the boundary between basement slice 'B4', of the northwestern domain, truncating the 'B3'+ 'C3' basement-cover pair in the eastern domain.

### ***Variation of D<sub>2</sub> strain in the Ptarmigan Fiord area and strain localization at basement-cover contacts***

Large variations in  $S_2$  foliation and lineation are documented in the rocks of the Ptarmigan Fiord area, from areas of relatively low strain where coarse-grained igneous textures and sedimentary structures (such as bedding, see Figure 3e) are preserved, to areas of high strain with strong  $D_2$



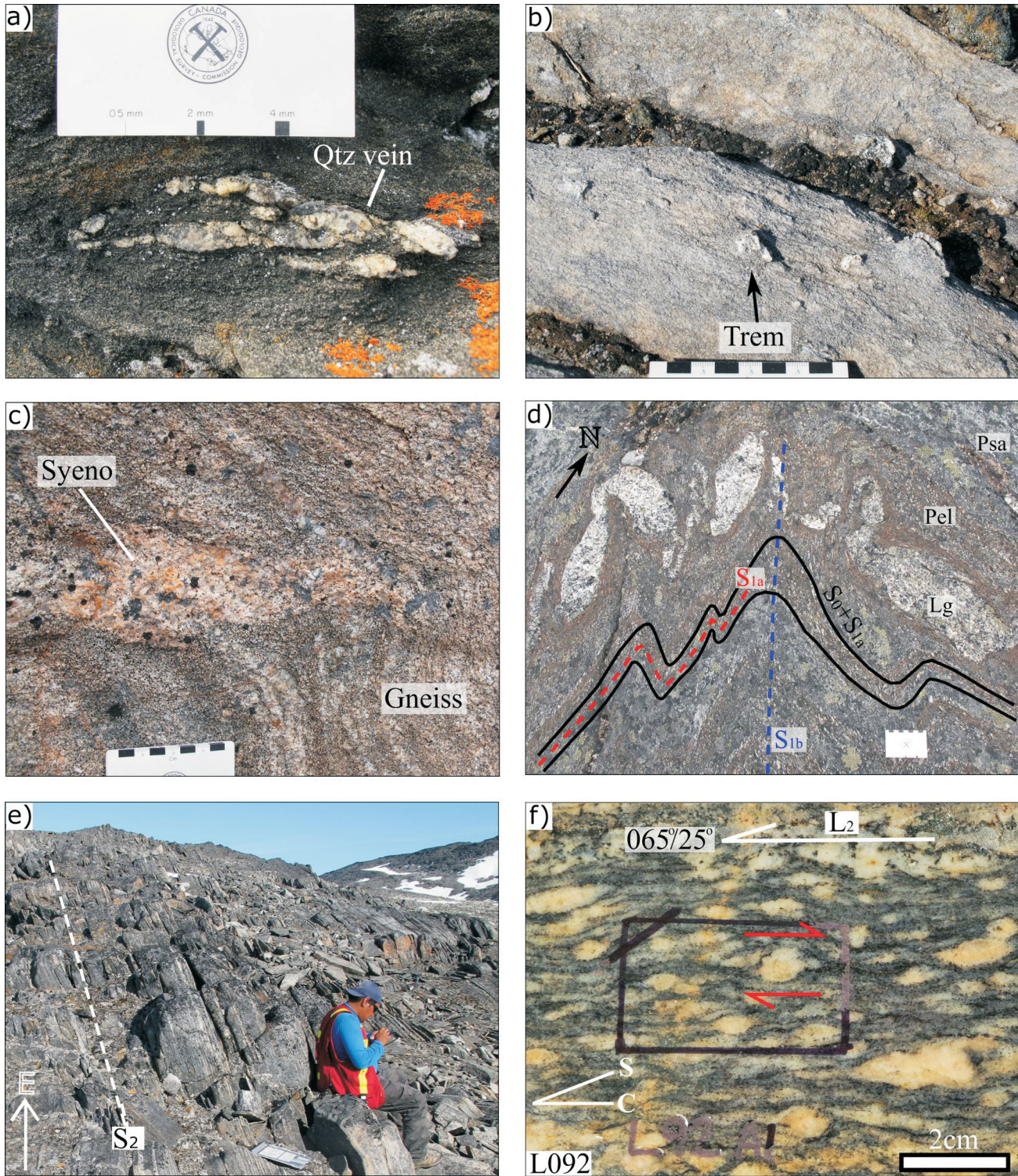


**Figure 4:** Lithology and structure, Ptarmigan Fiord, Hall Peninsula of Baffin Island: **a)** northwestward view of fine-grained garnet-biotite amphibolite with sheath-folded quartz vein; **b)** eastward view of calcisilicate with 2–5 cm size tremolite knots; **c)** northward view of weakly foliated syenogranite lens that crosscuts gneissic foliation in basement; **d)**  $S_{1a}$  compositional layering and foliation with concordant leucogranite or boudinaged veins folded by  $F_{1b}$  folds, resulting in the development of  $S_{1b}$  foliation; **e)** eastward view of  $S_2$  foliation in granodiorite basement (B1 imbricate); **f)** southeastward view of a slabbed granodiorite basement sample from outcrop L092. View is of the motion plane, cut parallel to  $L_2$  and perpendicular to  $S_2$ , exhibiting sigma ( $\sigma$ )-type K-feldspar porphyroclasts inclined to the foliation with top-to-the-southwest sense of shear. Abbreviations: Lg, leucogranite veins; Pel, pelitic schist; Psa, psammitic schist; Qtz, quartz; Syeno, syenogranite; Trem, tremolite; C, C-planes (cisaillement planes); S, S-planes (schistosité planes).



mineral and stretching lineations, and mylonitic textures, in all rock types.

In the eastern domain, autochthonous basement orthogneiss ('B0' in Figure 1), the deepest exposed structural levels in the area, contains large euhedral (~5–15 mm) phenocrysts and the preferred orientation of biotite and muscovite that forms a weak foliation. These are interpreted to be the lowest-strain plutonic rocks in the region and do not contain a visible mineral or stretching lineation, (Figure 3a). However, in the immediate vicinity of the contact with the overlying cover rocks (Figure 3c, 'C0' on Figure 1), platy minerals are aligned in a foliation; and euhedral phenocrysts, especially K-feldspar, occur as elongate porphyroclasts defining a weak stretching lineation (Figure 3b). These structures are interpreted as a strain gradient which may relate to minor shearing at the basement-cover contact. The pelitic and semipelitic rocks at the base of the cover sequence have a  $S_1$  foliation, and although it is aligned parallel to the  $S_2$  foliation in the underlying basement at contact, the rocks are interpreted to be low strain with respect to  $D_2$  deformation (Figure 3c). The basement-cover contact is therefore interpreted as a nonconformable contact between the 'B0' basement and overlying 'C0' supracrustal cover units, with only minor modification of strain.

The plutonic rocks at the base of the first basement imbricate ('B1' in Figure 1), contain a well-developed foliation as shown in Figure 4e. This foliation, interpreted as  $S_2$  in both the basement and 'C1' cover rocks, is defined by the re-alignment of gneissic banding and pre-existing  $S_1$  foliation into parallelism with the basement-cover contact. There appears to be an ~10 to 20% reduction in grain size in all basement units, as well as the development of mylonitic fabrics with shear-sense indicators in the motion-plane parallel to a dominant stretching lineation. Mineral and stretching lineations are penetrative, and are formed by quartz and feldspar rodding and aligned elongate sillimanite-quartz-K-feldspar knots. The strong  $S_2$  foliation,  $L_2$  mineral and stretching lineations and grain-size reduction indicate an increase in strain in the 'B1' basement imbricate, relative to the underlying 'B0' basement. The high-strain contact that separates basement-cover imbricates from the lower strain 'B0' and 'C0' rocks below them, can be interpreted as ductile thrust, where the transport direction was parallel to the mineral and stretching lineations.

At the base of the 'B2' and 'B3' basement imbricates (Figure 1), there is a further reduction in grain size, increase in the percentage of matrix grains and development of protomylonitic fabrics, similar to that of Figure 4f. Shear-sense indicators, in the form of sigma ( $\sigma$ ) and delta ( $\delta$ ) K-feldspar porphyroclasts, are used to determine the sense of motion parallel to the stretching lineation (as described in the next section). In finer grained rock types, the  $S_0$  gneissic

banding, which is re-aligned into the  $S_2$  shear foliation, shows evidence of extension parallel to the lineation in the form of pulled-apart mafic-mineral and biotite-rich layers (Figure 5a), and boudins.

Evidence for extension also occurs in the pelitic units in the form of large 1–2 m thick rose quartz lineation-parallel boudins. All of these structural observations at base of the 'B2' and 'B3' basement imbricates indicate increases in strain. Based on field observations of the eastern domain of the map area, it can be concluded that the bottom part of the basement slices in the basement-cover imbricates ('B1'+ 'C1' to 'B3'+ 'C3') represent moderate to steeply dipping ductile shear zones with  $T_{2a}$  thrust movement.

In the northwestern domain, the basement rocks at the base of the thrust imbricates ('B4', 'B5', 'B6' in Figure 1) typically show a further reduction in grain size and increase in the percentage of matrix, resulting in darker colour, and the development quartz- and feldspar-ribbon mylonite textures (Figure 5b). Mylonitic fabrics also occur in the northwestern part of the map area where the cover slices 'C4', 'C5' and 'C6' are truncated or pinched out, and shear zones delineate basement-on-basement contacts at the lower part of basement slice 'B4' and 'B5' (Figures 1, 5b). Northwest-trending sheath folds with ~50° plunges, defined by folded quartz veins, occur in the garnet-biotite amphibolite unit (Figure 4a) at the top of the supracrustal sequence in cover imbricate 'C4' (Figure 1). In cover slices from 'C2' to 'C6', the amphibolite is typically structurally overlain by basement imbricates. Perhaps the top of the relatively competent amphibolite served to localize deformation during overthrusting. Based on an increased percentage of matrix grains, general grain-size reduction and presence of mylonite and sheath folds, these rocks are interpreted to be the highest strain in the study area, and represent discrete ductile shear zones with  $T_{2c}$  thrust movement.

### ***Kinematic indicators: transport direction of ductile thrust faults***

The strained bases of basement slices within 'B1'+ 'C1' to 'B6'+ 'C6' basement-cover imbricates, and at the base of 'B7', are interpreted to represent ductile shear zones (thrust faults); and kinematic indicators are used to determine the sense of motion in the Ptarmigan Fiord area. Sigma ( $\sigma$ ) and delta ( $\delta$ ) shaped K-feldspar porphyroclasts within the basement gneiss, and macroscopic shear indicators defined by pulled-apart gneissic banding, are used as kinematic indicators. This section describes a number of shear-sense indicators that, in conjunction with strain variation, provide an explanation for the map patterns. The location of shear-sense indicators are shown on Figure 1 as station numbers in blue font (e.g., W018).

Data in the eastern domain are presented from south to north. Station C055, in 'B2', is located on the southern limb



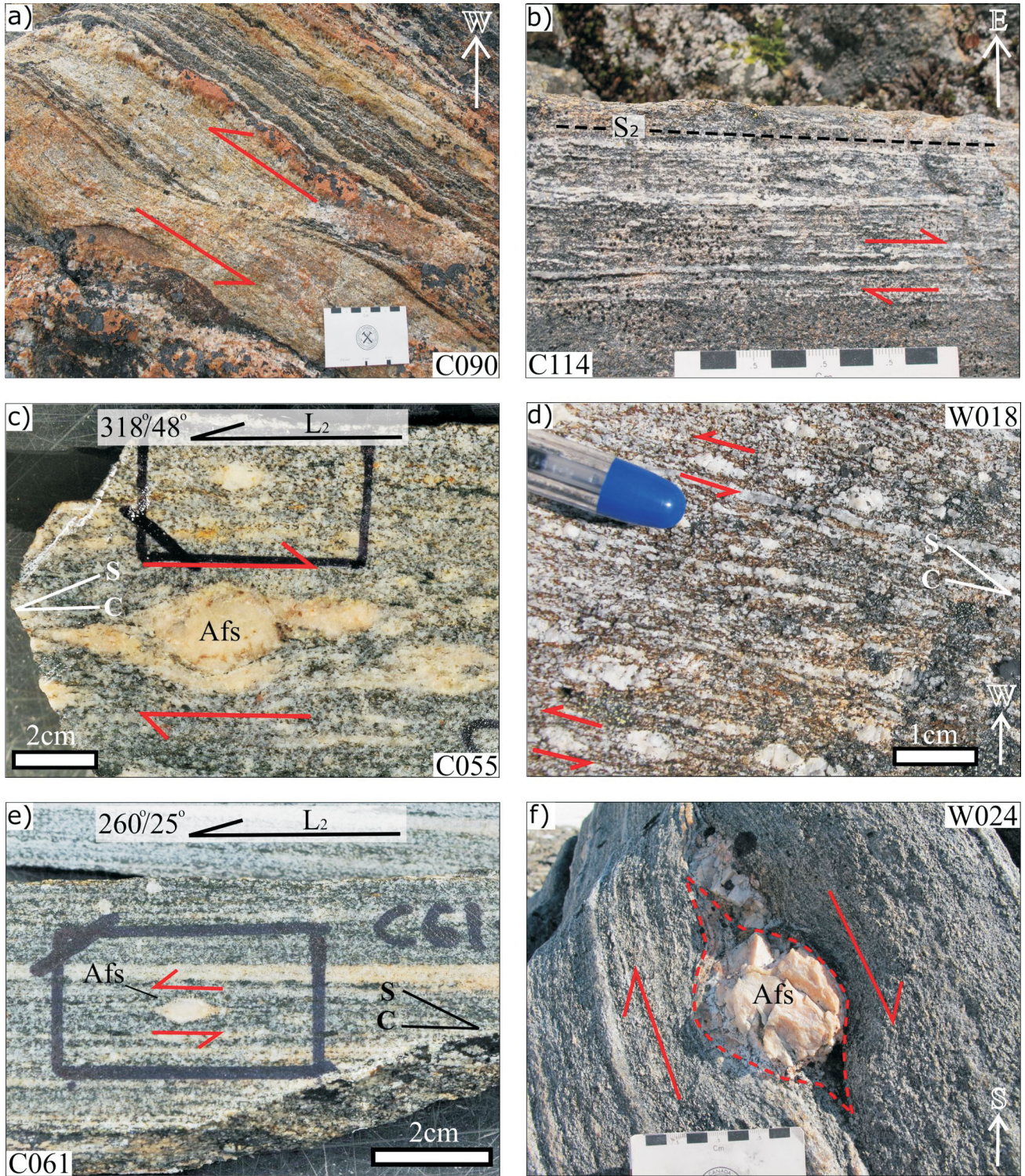


**Figure 5:** Photographs of structures in the Ptarmigan Fiord area, Hall Peninsula of Baffin Island: **a)** westward view of top-up-to-the-south (reverse shear sense) macroscopic shear-sense indicator defined by extension of a biotite-rich layer in gneissic granodiorite basement, (station C090); **b)** trace of quartz and feldspar ribbons in mylonite in basement-on-basement thrust contact in granodiorite (station C114); **c)** sigma ( $\sigma$ )-type porphyroclast in 'B2' basement granodiorite showing apparent reverse (top-to-the-south) sense of shear (station C055); **d)** sigma ( $\sigma$ )-type porphyroclasts showing apparent reverse (top-to-the-southeast) sense of shear in 'B1' granodiorite basement (station W018, pen parallel to lineation); **e)** sigma ( $\sigma$ )-type porphyroclast within 'B2' basement granodiorite showing apparent normal (top-to-the-west) sense of shear at station C061; **f)** sigma ( $\sigma$ )-type porphyroclast in 'B3' basement granodiorite showing apparent normal (top-to-the-west) sense of shear (station W024).



of the upright  $F_{2b}$  synclinal keel. At this station, a basement granodiorite contains a lineation trending northwest and plunging  $48^\circ$ , with  $\sigma$ -type porphyroclast indicating an apparent reverse or top-to-the-southeast sense of shear (Figure 5c). This same shear sense also occurs in a structurally lower basement imbricate ('B1') on the southern limb of the  $F_{2b}$  synclinal keel, at station W018. Here, finer grained  $\sigma$ -type porphyroclast shear indicators, aligned parallel to a north-trending lineation with a plunge of  $44^\circ$  also showed a top-to-the-south reverse shear sense (Figure 5d). Based on these two shear indicators from the southern half of the synclinal keel, the inferred direction of thrusting is roughly south, with an apparent reverse sense of shear; this is consistent with interpretations in the region (Dyck and St-Onge, 2014).

In contrast, at station C061 in 'B2', on the northern limb of the upright  $F_{2b}$  synclinal keel, the mineral and stretching lineation trends west and plunges shallowly at  $20^\circ$ , with a  $\sigma$ -type porphyroclast indicating a normal, top-to-the-west shear sense (Figure 5e). Farther west, station W024 located on a structurally higher basement imbricate ('B3') also has a west-trending lineation plunging shallowly at  $\sim 30^\circ$ . The shear sense at this station is also top-to-the-west, normal sense of shear, as indicated by a large  $\sigma$ -type K-feldspar porphyroclast within granodiorite (Figure 5f). Based on these two shear indicators from the northern half of the synclinal keel, the inferred direction of transport is roughly west, with an apparent normal sense of shear. One of the primary objectives of the M.Sc. thesis will be to determine the primary orientation of the  $T_{2a}$  thrusts by unwinding the  $S_{2b}$  folding.

In the northwestern part of the map area, at station C090 in 'B4', a macroscopic shear-sense indicator, defined by the extension of a biotite-rich layer in a gneissic basement unit, is aligned parallel to a roughly north-plunging lineation (Figure 5a). This kinematic indicator represents a top-to-the-south reverse sense of shear. This same shear sense was also recognized in structurally higher thrust imbricates at stations C114 and L092 in 'B4' and 'B5', respectively. Both of these stations have roughly north-plunging lineations, and shear indicators that recorded a top-to-the-south or thrust shear sense. Stations L092 (Figure 4f) and C114 (Figure 5b) are located along high-strain contacts, as described in the previous section, interpreted as basement-on-basement ductile thrusts. Based on these observations, the shear indicators found in the northwestern domain of the map area, at the base of the basement slices in basement-cover imbricates ('B4'+ 'C4' to 'B7'), represent south-directed thrust faults.

## Conclusions

The  $D_1$  event (Table 1), involving east-west crustal shortening (pre-synthermal peak) is manifest in the supracrustal

rocks as a strong foliation ( $S_{1a}$ ) that formed during thermal peak amphibolite-facies metamorphism. The  $S_{1a}$  foliation and  $S_0$  primary bedding in metasedimentary rocks were re-folded by  $F_{1b}$  folds, and a cleavage ( $S_{1b}$ ) developed axial planar to the  $F_{1b}$  folding.

The  $D_2$  event, involving southeast-northwest crustal shortening (post-thermal peak), is recorded in the basement and supracrustal rocks by  $T_2$  thick-skin thrusting with dominantly south- to southeast-directed thrust motion. The  $T_2$  thrust imbricates can be identified on the basis of the following observations and interpretations: 1) the contact between autochthonous basement rocks 'B0' and the cover stratigraphy 'C0' is low-strain and is interpreted as a nonconformable contact, and 2) the contacts between the supracrustal rocks and the structurally overlying basement orthogneiss are higher-strain, and correspond to localized shear zones at the base of each 'B1+C1' to 'B6+C6' basement-cover couplet and at the base of 'B7'. The  $T_2$  ductile shear zones, interpreted as thrusts, were responsible for the development of the  $L_2$  mineral and stretching lineations and  $S_2$  mylonitic foliations. The  $D_2$  deformation can be characterized with respect to an eastern domain and a northwestern domain of the map area, both structurally underlain by autochthonous 'B0+C0' in the south (Figure 1). In the eastern domain, the map pattern is dominated by the keel of an  $F_{2b}$  syncline that folds basement-cover  $T_{2a}$  thrust imbricates ('B0'+ 'C0' to 'B3'+ 'C3'). The map pattern of the northwestern domain is characterized by a generally north- to northwest-dipping panel of basement and cover ('B4'+ 'C4' to 'B7') imbricates separated by  $T_{2c}$  thrusts. At the boundary between the northwestern structural domain and the eastern domain, a stack of basement-cover thrust imbricates ( $T_{2c}$ ), with 'B4' at the base, truncate  $T_{2a}$  basement-cover imbricates ('B3'+ 'C3' and 'B2'+ 'C2') of the eastern domain (Figure 2b). The crosscutting relationship implies that the  $T_{2c}$  thrust fault at the base of the 'B4' basement imbricate is younger than the  $T_{2a}$  thrusts and the  $F_{2b}$  fold. This crosscutting relationship implies a two-stage  $D_2$  event involving thrusting of the  $T_{2a}$  imbricates first, then folding of the  $T_{2a}$  imbricates before truncation by  $T_{2c}$  thrust imbricates.

A regional  $D_3$  event (Table 1) has been described in the Hall Peninsula (Steenkamp and St-Onge, 2014; Dyck and St-Onge, 2014). In the Ptarmigan Fiord area, open upright folding ( $F_3$ ) of the  $D_2$  map-scale patterns is interpreted as  $D_3$ . In the northwestern domain,  $F_3$  folding resulted in gentle buckling of the  $T_{2c}$  thrust imbricates, while in the eastern domain  $F_3$  folding resulted in a gentle bend of the synclinal keel in the eastern domain of the study area (Figure 1).

The M.Sc. research of T. Chadwick is directed toward detailed petrographic, structural, microstructural and kinematic studies of samples and field data; construction of cross sections; and, map- and regional-scale structural

analysis (e.g., is the thrust at the base of 'B4' an out of sequence thrust?). Goals are to document the geometry and structural evolution of the Ptarmigan Fiord area and to use the results to constrain the geological and structural history of the Hall Peninsula.

## Economic considerations

The geological framework and structural evolution of the Ptarmigan Fiord area may have implications for the distribution of mineral resources in the eastern Baffin Island region. Kimberlite pipes, which are geological conduits for transporting diamonds to the Earth's surface, are known to occur in the Archean basement south of Ptarmigan Fiord. This study offers the potential to understand how the emplacement of kimberlite pipes may have been affected by prior imbrication of crystalline basement. A better understanding of the crustal architecture of the Ptarmigan Fiord area could also reveal the full extent of crystalline basement in this part of the eastern Arctic and potentially aid exploration companies in their search for new diamond occurrences in Nunavut.

## Acknowledgments

The authors thank D. Liikane, T. Milton, S. Noble-Nowdluk, T. Rowe and A. Ford for providing enthusiastic field assistance and valuable discussions. The Geo-mapping for Energy and Minerals (GEM) program provided financial support for this work. We also thank H. Steenkamp for organizing thin sections for future work through Strategic Investments in Northern Economic Development (SINED) program offered by Canadian Northern Economic Development Agency (CanNor).

Natural Resources Canada, Earth Sciences Sector contribution 20150289

## References

Blackadar, R.G. 1967: Geological reconnaissance, southern Baffin Island, District of Franklin; Geological Survey of Canada, Paper 66-47, 32 p.

Corrigan, D. 2012: Paleoproterozoic crustal evolution and tectonic processes: insights from LITHOPROBE program in the Trans-Hudson orogen, Canada; Chapter 4 in *Tectonic Styles in Canada: The LITHOPROBE Perspective*, J.A. Percival, F.A. Cook and R.M. Clowes (ed.), Geological Association of Canada, Special Paper 49, p. 237–284.

Dyck, B.J. and St-Onge, M.R. 2014: Dehydration-melting reactions, leucogranite emplacement and the Paleoproterozoic structural evolution of Hall Peninsula, Baffin Island, Nunavut; *in Summary of Activities 2013*, Canada-Nunavut Geoscience Office, p. 73–84.

From, R.E., St-Onge, M.R. and Camacho A. 2014: Preliminary characterization of the Archean orthogneiss complex of Hall Peninsula, Baffin Island, Nunavut; *in Summary of Activities 2013*, Canada-Nunavut Geoscience Office, p. 47–56.

Hoffman, P.F. 1988: United Plates of America, the birth of a craton: Early Proterozoic assembly and growth of Laurentia; *Annual Review of Earth and Planetary Sciences*, v. 16, p. 543–603.

Lewry, J.F. and Collerson, K.D. 1990: The Trans-Hudson Orogen: extent, subdivisions and problems; *in The Early Proterozoic Trans-Hudson Orogen of North America*, J.F. Lewry and M.R. Stauffer (ed.), Geological Association of Canada, Special Paper 37, p. 1–14.

MacKay, C.B., Ansdell, K.M., St-Onge, M.R., Machado, G. and Bilodeau, C. 2013: Geological relationships in the Qaqqanittuaq area, southern Hall Peninsula, Baffin Island, Nunavut; *in Summary of Activities 2012*, Canada-Nunavut Geoscience Office, p. 55–64.

MacKay, C.B. and Ansdell, K.M. 2014: Geochemical study of mafic and ultramafic rocks from southern Hall Peninsula, Baffin Island, Nunavut; *in Summary of Activities 2013*, Canada-Nunavut Geoscience Office, p. 85–92.

Rayner, N.M. 2014: New uranium-lead geochronological results from Hall Peninsula, Baffin Island, Nunavut; *in Summary of Activities 2013*, Canada-Nunavut Geoscience Office, p. 39–46.

Scott, D.J. 1999: U-Pb geochronology of the eastern Hall Peninsula, southern Baffin Island, Canada: a northern link between the Archean of West Greenland and the Paleoproterozoic Torngat Orogen of northern Labrador; *Precambrian Research*, v. 93, p. 5–26.

Steenkamp, H.M. and St-Onge, M.R. 2014: Overview of the 2013 regional bedrock mapping program on northern Hall Peninsula, Baffin Island, Nunavut; *in Summary of Activities 2013*, Canada-Nunavut Geoscience Office, p. 27–38.

St-Onge, M.R., Searle, M.P. and Wodicka, N. 2006: Trans-Hudson Orogen of North America and Himalaya–Karakorum–Tibetan Orogen of Asia: structural and thermal characteristics of the lower and upper plates; *Tectonics*, v. 25, p. 1–22, doi: 10.1029-2005TC001907

St-Onge, M.R., Wodicka, N. and Ijewliw, O. 2007: Polymetamorphic evolution of the Trans-Hudson Orogen, Baffin Island, Canada: integration of petrological, structural and geochronological data; *Journal of Petrology*, v. 48, p. 271–302.

St-Onge, M.R., Van Gool, J.A.M., Garde, A.A. and Scott, D.J. 2009: Correlation of Archean and Palaeoproterozoic units between northeastern Canada and western Greenland: constraining the pre-collisional upper plate accretionary history of the Trans-Hudson orogen; *Geological Society, London, Special Publication 318*, p. 193–235.

Weller, O.M., Dyck, B.J., St-Onge, M.R., Rayner, N.M. and Tschirhart, V. 2015: Completing the bedrock mapping of southern Baffin Island, Nunavut: plutonic suites and regional stratigraphy; *in Summary of Activities 2015*, Canada-Nunavut Geoscience Office, p. 33–48.